Electronic Supplementary Material (ESI) for Journal of Materials Chemistry C.
This journal is © The Royal Society of Chemistry 2020

Supporting information

Anchoring of $CsPbBr_3$ Perovskite Quantum Dots on BN Nanostructures for Enhanced Efficiency and Stability: A Comparison Study

Mengmeng Yu [a,b], Xin He [a,b,c], Danyang Li [a,b], Jing Lin [a,b,*], Chao Yu [a,b], Yi Fang [a,b], Zhenya Liu [a,b], Zhonglu Guo [a,b], Yang Huang [a,b,*] Chengchun Tang [a,b]

[a] School of Materials Science and Engineering, Hebei University of Technology, Tianjin 300130, P. R. China

[b] Hebei Key Laboratory of Boron Nitride Micro and Nano Materials, Hebei University of Technology, Tianjin 300130, P. R. China

[c] School of Mechanical and Energy Engineering, HuangHuai University, Henan 463000, P. R. China

* Corresponding author. E-mail: huangyang@hebut.edu.cn (Y. H.); linjing@hebut.edu.cn (J. L.)

Synthesis of BN nanosheets (BNNS): Boric acid and urea with a molar ratio of 1:48 were dissolved in 40 mL of deionized water and heated at 65°C, until the water was completely evaporated. The dried mixtures were heated at 1100°C for 5 hours in a N_2 atmosphere, and BNNS were successfully obtained [1].

Synthesis of BN nanofibers (BNNF): In a classical synthesis, 4.64 g of H_3BO_3 and 3.15 g of $C_3N_6H_6$ were dissolved in 250 mL of deionized water and heated at 90°C for 4 hours to obtain the hot aqueous solution. Subsequently, the white precursor was obtained by freezing the hot water solution with liquid nitrogen and freeze-drying in vacuum for 7-8 days. The white precursor was heated at 1050°C for 4 hours in a N_2 atmosphere, and BNNF were successfully obtained [2].

Synthesis of BN nanoparticles (BNNP): It was calcined at 1500°C with trimethyl borate and ammonia gas as boron source and nitrogen source respectively [3].

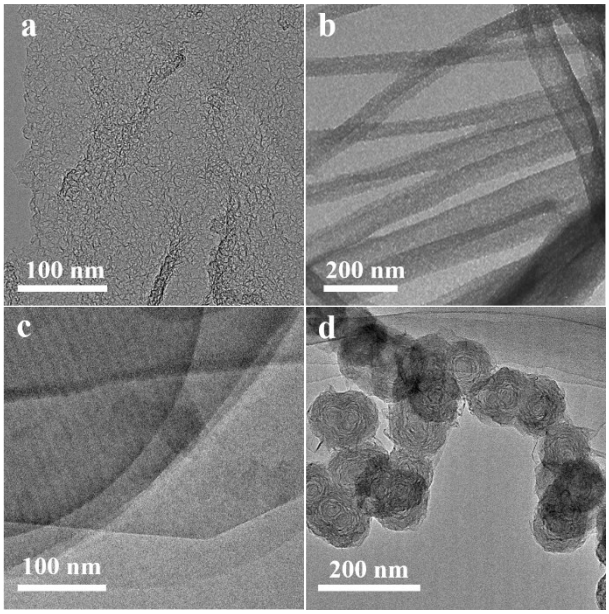

Figure S1. TEM images of BNNS (a), BNNF (b), C-BNNS (c) and BNNP (d).

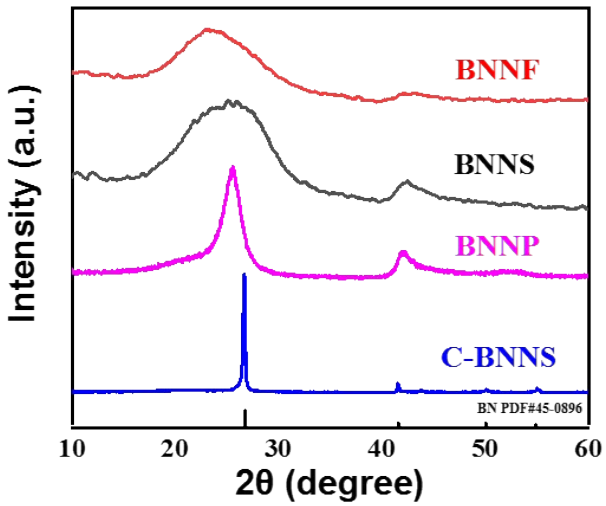

Figure S2. XRD patterns of BNNS, BNNF, C-BNNS and BNNP.

All the BN samples have shown diffraction peaks at 2θ = 21-27° and 2θ = 42-44°, which are attributed to (002) and (110) crystal planes of hexagon BN (h-BN), respectively. For commercial nanosheets (C-NNS), the sharp and intense diffraction peaks indicate its highest degree of crystallization among the four kinds of BN materials. The highly ordered (002) layers with small d_{0002} distances is similar with bulk h-BN. While for the BNNP, BNNS and BNNF samples, the obviously broadened diffraction peak with less intense imply the partially disordered BN phases existing. Especially, the gradually blue shift of (002) peak indicates the value of d_{0002} increases as compared with C-BNNS sample, revealing turbostratic BN phase of the samples. The difference of XRD results in BN samples is due to the C and O related impurities existing in the porous nanofibers, nanosheets and nanospheres [2].

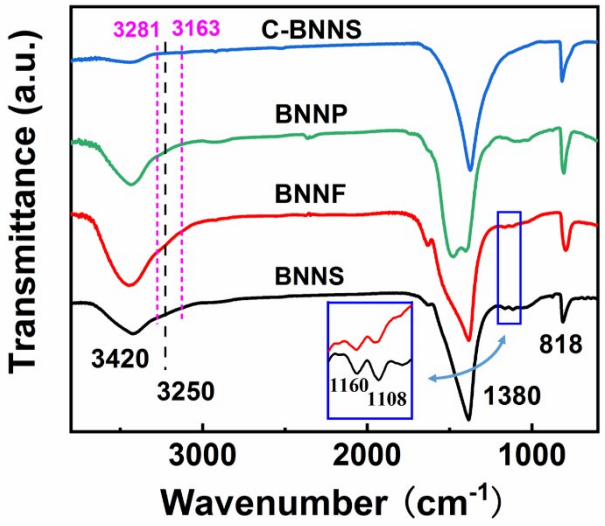

Figure S3. FTIR spectra of BNNS, BNNF, C-BNNS and BNNP.

All BN samples show two absorption bands at 1380 and 818 cm^{-1}, which can be attributed to B-N tensile vibration and B-N-B bending vibration, respectively. The peaks at 3420 and 3250 cm^{-1} are due to B-OH and B-NH_2 stretching vibrations. In particular, the red shift of the adsorption edge move from 3281 to 3163 cm^{-1}, indicating that the –NH_2 and –OH vibrations in BNNS, BNNF, and BNNPs increase compared to C-BNNS [4]. The occurrence of these vibrations may be related to the incorporation of impurities and defects in BNs. In addition, in BNNS and BNNF, the additional peaks at 1160 (B-N-O) and 1108 cm^{-1} (BOH) indicate an abundance of functional groups on the surface.

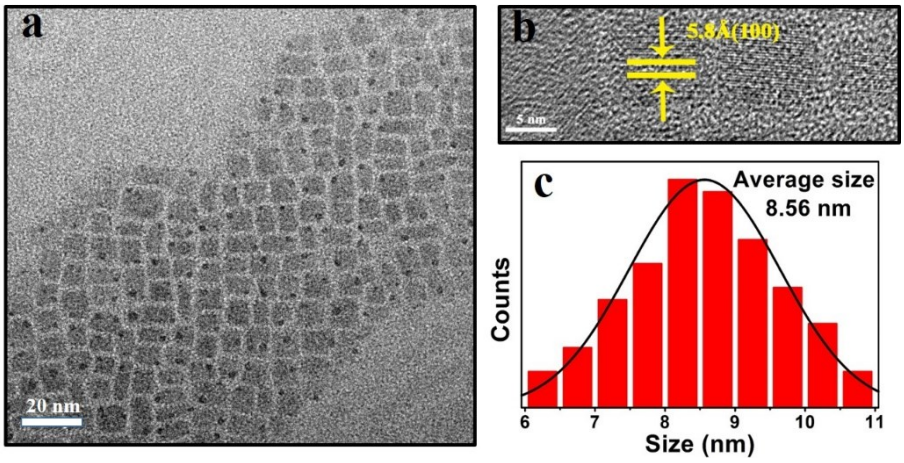

Figure S4. (a) TEM image, (b) HRTEM image, and (c) PSD of prepared CPB QDs.

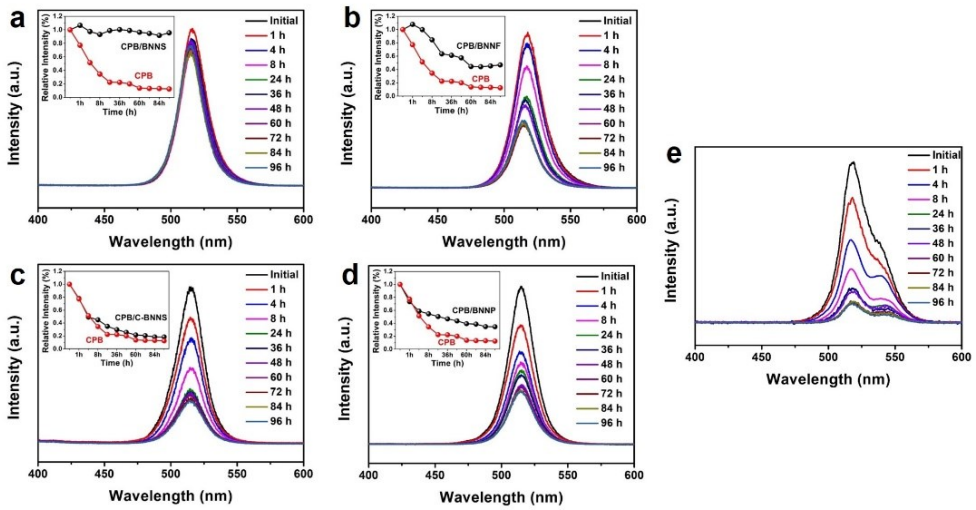

Figure S5. Photostability tests of the nanocomposites. (a-e) PL emission spectra of CPB/BNNS (a), CPB/BNNF (b), CPB/C-BNNS (c), CPB/BNNP (d) composite powders measured under 96 hours of continuously exposure to UV light. (Insets) normalized PL intensity as a function of UV exposing time. (e) PL emission spectra of pure CPB QDs powders measured under 96 hours of continuously exposure to UV light.

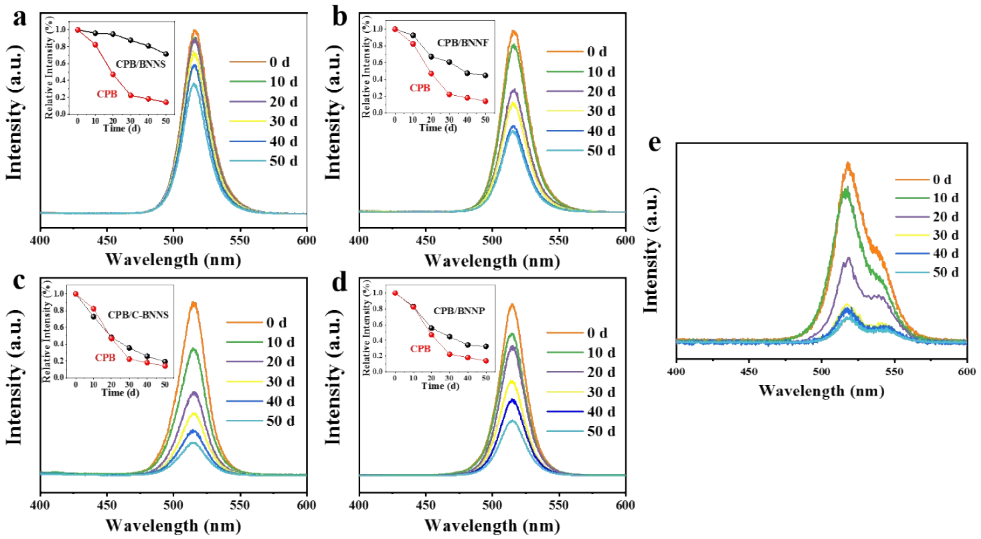

Figure S6. Long-term storage stability tests of the nanocomposites. (a-e) PL emission spectra of CPB/BNNS (a), CPB/BNNF (b), CPB/C-BNNS (c), CPB/BNNP (d) composite powders measured under 50 consecutive days of exposure to the atmosphere. (Insets) normalized PL intensity as a function of storage time. (e) PL emission spectra of pure CPB QDs powders measured under 50 consecutive days of exposure to the atmosphere.

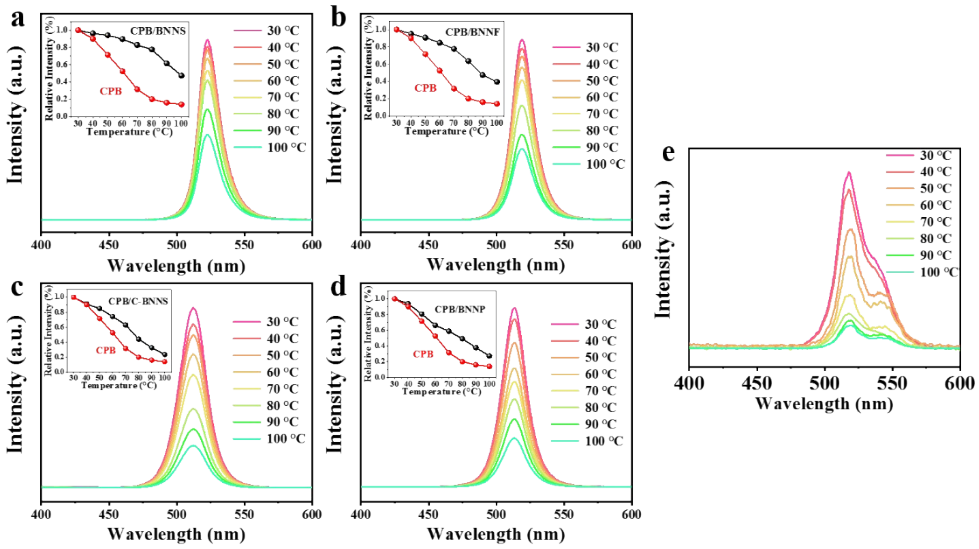

Figure S7. Thermal stability tests of the nanocomposites. (a-e) PL emission spectra of CPB/BNNS (a), CPB/BNNF (b), CPB/C-BNNS (c), CPB/BNNP (d) composite powders measured under elevated ambient temperatures range from 30 to 100°C. (Insets) normalized PL intensity as a function of experimental temperature. (e) PL emission spectra of pure CPB QDs powders measured under elevated ambient temperatures range from 30 to 100°C.

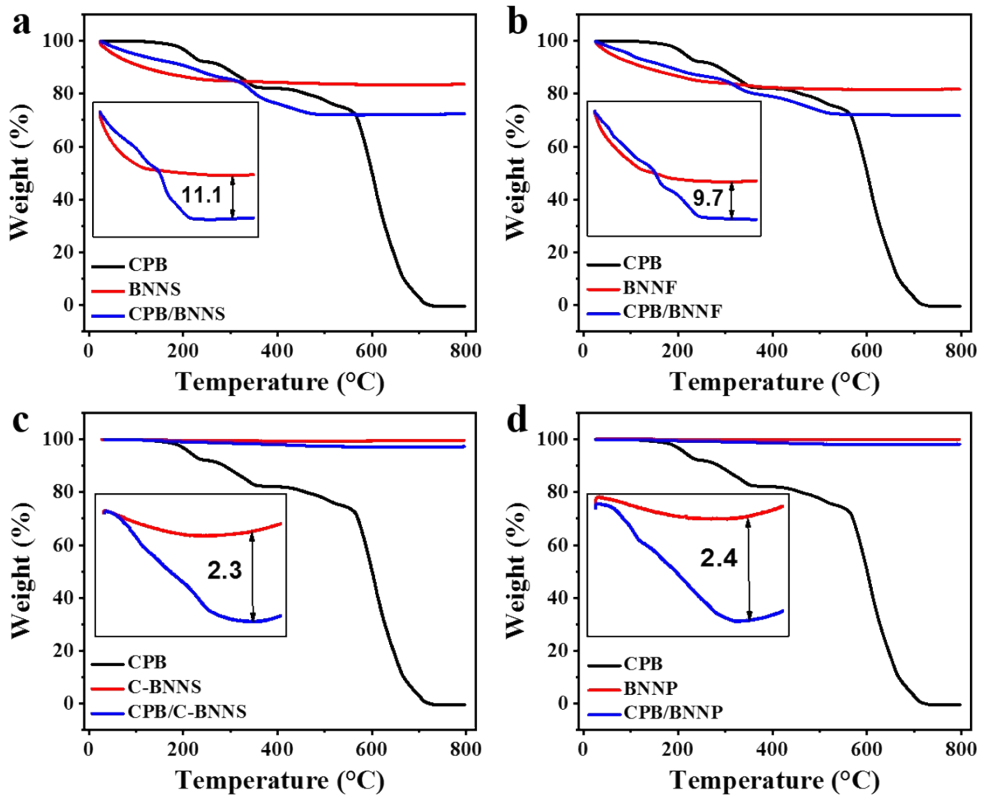

Figure S8. TG curves of pure CPB QDs, pure BNs and different CPB/BN nanocomposites. (Insets) only BN and its corresponding composites TG picture.

The relative contents of $CsPbBr_3$ QDs on BN materials were analyzed by thermogravimetric (TG) measurement. The weight loss of pure $CsPbBr_3$ QDs at 800°C is almost 100 wt% (black lines), indicating that the QDs have been completely decomposed at high temperature. The difference in weight loss between the composite material (blue lines in each figure) and the corresponding pure BN at 800°C (red lines) can be expressed as the relative amount of QDs adsorbed on the BN supporting (inset). From the above analysis, we can conclude that the relative contents of QDs loaded on BNNS and BNNF are much higher than that of C-BNNS and BNNP.

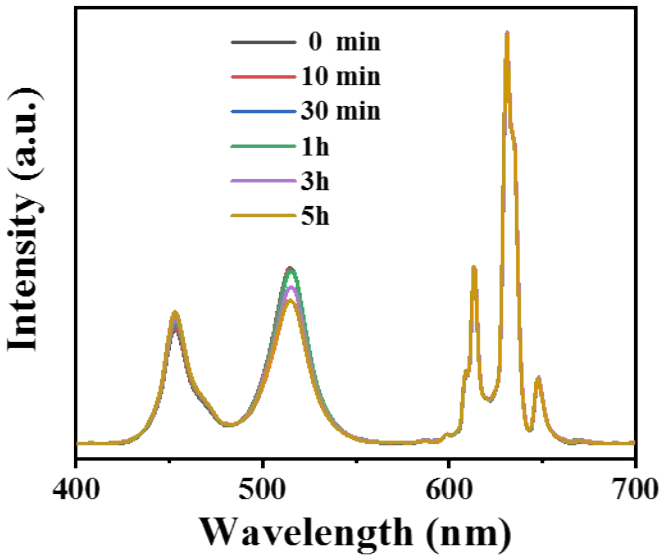

Figure S9. The relationship between the luminous intensity of the white LED device and the working time.

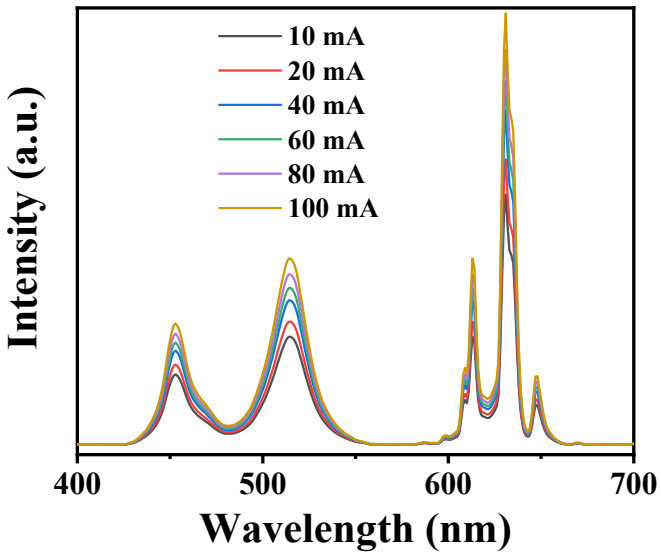

Figure S10. The emission spectrum of the white LED device measured under different operating currents.

References

1. A. Nag, K. Raidongia, K. P. S. S. Hembram, R. Datta, U. V. Waghmare and C. N. R. Rao, *ACS Nano*, 2010, **4**, 1539-1544.

2. J. Lin, L. Xu, Y. Huang, J. Li, W. Wang, C. Feng, Z. Liu, X. Xu, J. Zou and C. Tang, *RSC Adv.*, 2016, **6**, 1253-1259.

3. C. Tang, Y. Bando, Y. Huang, C. Zhi and D. Golberg, *Adv. Funct. Mater.*, 2008, **18**, 3653-3661.

4. C. Cao, Y. Xue, Z. Liu, Z. Zhou, J. Ji, Q. Song, Q. Hu, Y. Fang and C. Tang, *2D Mater.*, 2019, **6**, 035014-035023.